Negative refraction of acoustic waves using a foam-like metallic structure

Anne-Christine Hladky, Jerome O. Vasseur, G. Haw, Charles Croënne, L. Haumesser, A.N. Norris

AIP | Applied Physics Letters

Negative refraction of acoustic waves using a foam-like metallic structure

A.-C. Hladky-Hennion, J. O. Vasseur, G. Haw, C. Croënne, L. Haumesser et al.

Citation: Appl. Phys. Lett. **102**, 144103 (2013); doi: 10.1063/1.4801642
View online: http://dx.doi.org/10.1063/1.4801642
View Table of Contents: http://apl.aip.org/resource/1/APPLAB/v102/i14
Published by the American Institute of Physics.

Negative refraction of acoustic waves using a foam-like metallic structure

A.-C. Hladky-Hennion,[1] J. O. Vasseur,[1] G. Haw,[1] C. Croënne,[2] L. Haumesser,[3] and A. N. Norris[4]
[1]*Institut d'Electronique, de Microélectronique et de Nanotechnologie (IEMN, UMR CNRS 8520), 41 Boulevard Vauban, 59046 Lille, France*
[2]*Department of Physics and Materials Science, City University of Hong Kong, Tat Chee Avenue, Kowloon Tong, Kowloon, Hong Kong*
[3]*Groupe de Recherche en Matériaux, Microélectronique, Acoustique et Nanotechnologies (GREMAN, UMR CNRS 7347), rue de la chocolaterie, 41000 Blois, France*
[4]*Department of Mechanical and Aerospace Engineering, Rutgers University, Piscataway, New Jersey 08854, USA*

(Received 31 January 2013; accepted 27 March 2013; published online 9 April 2013)

A phononic crystal (PC) slab made of a single metallic phase is shown, theoretically and experimentally, to display perfect negative index matching and focusing capability when surrounded with water. The proposed PC slab is a centimeter scale hollow metallic foam-like structure in which acoustic energy is mediated via the metal lattice. The negative index property arises from an isolated branch of the dispersion curves corresponding to a mode that can be coupled to incident acoustic waves in surrounding water. This band also intercepts the water sound line at a frequency in the ultrasonic range. The metallic structure is consequently a candidate for the negative refraction of incident longitudinal waves. © *2013 AIP Publishing LLC*. [http://dx.doi.org/10.1063/1.4801642]

Acoustic wave propagation in man-made periodic composite materials, i.e., phononic crystals (PCs), may exhibit unusual properties[1] absent in natural materials. For example, under certain conditions Bragg scattering can produce large band gaps in which the propagation of elastic waves is forbidden. Many possible applications of PCs have been proposed based on this spectral property.[2] Associated band folding effects can lead to pass band branches with negative slope, i.e., phase and group velocity vectors in opposite directions, and consequently the PC behaves as an effective medium possessing a negative index of refraction. Negative refraction in PCs has been investigated theoretically and experimentally over the last ten years for its potential application in focusing acoustic or elastic waves at wavelength scale. Most of the studies were initially devoted to PCs with a fluid (liquid or air) matrix surrounding solid inclusions, in which only longitudinal waves propagate.[3–10] Negative index PCs may allow the realization of a flat super-lens able to focus acoustic waves with a resolution lower than the diffraction limit.[5] The super-resolution has been achieved, for example, using a PC lens made of a triangular array of steel cylinders immersed in methanol and surrounded with water.[6] PC superlenses should lead to enhancement of the resolution of near-field medical imaging and of the efficiency of ultrasonic therapy devices.[11] For this kind of applications, it seems necessary to consider a composite structure that can be easily handled, and this requires considering PCs with a solid matrix rather than PCs with a fluid matrix. Negative refraction phenomena in PCs made of solid matrices are more complex than in fluid matrix PCs due to the coexistence of waves of different polarizations (longitudinal and transverse waves).[12,13]

Such possible medical applications of PC superlenses require that (1) the PC is made of a solid matrix, (2) the PC is surrounded with a biological fluid like water, (3) the negative refraction and then the focusing phenomenon involve longitudinal waves, and (4) simultaneous impedance and phase speed matching occur. In a recent paper,[14] theoretical and experimental evidences of negative refraction of a longitudinal elastic wave in a triangular array of steel rods inserted in an epoxy block were reported. This structure suffers from a poor phase velocity matching with surrounding water (an equivalent index of −0.26 with respect with water at ultrasonic frequencies) and is not suitable for focusing applications. With the aim of enhancing the coupling between surrounding water and a solid PC, a structure originally proposed by Norris *et al.*[15] for acoustic cloaking purposes is investigated here. This structure is an aluminum-based metallic foam whose effective density and bulk modulus are equivalent to those of water in the long wavelength limit, i.e., in *the quasi-static regime*, and therefore is commonly named metal water structure (MWS). Due to a very low shear modulus, shear vibration modes occur at very low frequency and do not affect acoustic wave propagation significantly at higher frequencies. The low shear rigidity is designed to make the structure behave like a 2D pentamode material, which is desirable for its acoustic cloaking potential.[16] Here we are concerned with the higher frequency property of the MWS exhibiting a negative refraction dispersion branch that can be coupled with incident longitudinal waves. In this letter, we demonstrate that a MWS flat lens displays perfect refractive index matching with surrounding water and exhibits the focusing capability. Experimental results obtained in the ultrasonic frequency domain and showing an overall agreement with the theoretical predictions based on the finite element method are presented.

The MWS in the (xOy) plane is a two-dimensional network of metallic arms arranged in a regular honeycomb lattice (Fig. 1(a)), assumed to be infinite in the z direction. The 3-arm stars located at the vertices of the hexagons play the role of additional masses. These masses primarily control the effective density of the MWS, whereas the interconnecting

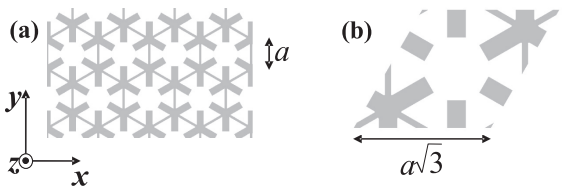

FIG. 1. (a) Schematic description of the foam-like metallic structure: honeycomb lattice with additional masses on the corners and (b) corresponding unit cell used for FEM calculation.

arm thickness mainly governs its effective elasticity.[15] The whole structure is made of aluminum,[17] permeated by air. The width of the interconnecting arms, the width and the length of the star arms, and the sides of the regular hexagon are $\ell = 0.5\,\text{mm}$, $\ell' = 1.51\,\text{mm}$, $h = 3.02\,\text{mm}$, and $a = 6.445\,\text{mm}$, respectively. These geometrical characteristics ensure[15] that the effective density, bulk modulus, and shear modulus of the MWS in the *quasi-static regime* are 1000 kg m^{-3}, 2.25 GPa, and 0.065 GPa, respectively, very close to those of water. The MWS is perfectly periodic in the (xOy) plane with an elementary cell of parallelogram shape as shown in Fig. 1(b). The lattice parameter which corresponds to the sides of the elementary cell is $b = a\sqrt{3} = 11.16\,\text{mm}$. The aluminum filling fraction is about 37%. Dispersion curves for the infinite MWS were calculated using the finite element (FE) method[18] by meshing only the solid part of the parallelogram elementary cell, using periodic boundary conditions.

Figure 2(a) shows the band structure along the ΓJX path of the irreducible Brillouin zone. A branch with a negative slope is observed in the frequency range of 70, 80 kHz, corresponding to a vibrational mode of the MWS that can easily couple to an incident longitudinal wave in an external fluid medium such as water. The blue sonic line, which is the dispersion curve in water,[17] intersects the negative branch at two slightly different frequencies, namely, 70.8 kHz along the ΓJ direction and 71.6 kHz along the ΓX direction. The small difference in frequency indicates a slight anisotropy of the acoustic wave propagation through the MWS which may influence the focusing of the water/MWS/water system. Indeed, focusing by a PC superlens requires the "All Angle Negative Refraction" criterion to be satisfied,[5] i.e., the phase velocities in the PC and external water medium must match for all angles of incidence, and consequently the equifrequency contour (EFC) has to be circular. Figures 2(b)–2(d) show the EFCs in the MWS and in water at three nearby frequencies, 70.8, 71.2, and 71.6 kHz. While the sonic line intersects the dispersion curve along the ΓJ direction at 70.8 kHz, this frequency lies in a local stop band along the ΓX direction. Figure 2(b) shows that phase velocity matching is not satisfied for all angles of incidence. At 71.6 kHz (Fig. 2(d)) the EFC is approximately circular but with a smaller radius than water. The EFC at 71.2 kHz (Fig. 2(c)) is not exactly circular but is closer to that of water. Therefore, in the following simulations, the frequency of the incident longitudinal wave is fixed to 71.2 kHz.

The coupling efficiency with water and focusing capability of a MWS slab were investigated theoretically. The slab is 6-cell thick, large enough (32-cell wide) to avoid edge effects, and sandwiched between water regions. A source emitting cylindrical waves in the xOy plane at 71.2 kHz is located below the slab, and the focusing effect is observed above the MWS lens (Fig. 3). The amplitude of the pressure field around the slab is shown in Fig. 3 where a focusing effect is clearly visible. The amplitude of the image spot is about 6% of the source amplitude. The amplitude loss between the source and the image can be ascribed to an effective impedance mismatch between MWS and water. This is not surprising, since the operation frequency of 71.2 kHz is far from the *quasi-static regime*, and so the effective physical properties of the MWS are bound to differ from those of water.

The distance between the point source and the image spot is 115.5 mm, i.e., twice the slab thickness, if we consider an effective thickness of 6 row separations ($6\sqrt{3}b/2 = 9a$). This result is consistent with the value of -1 for the effective index

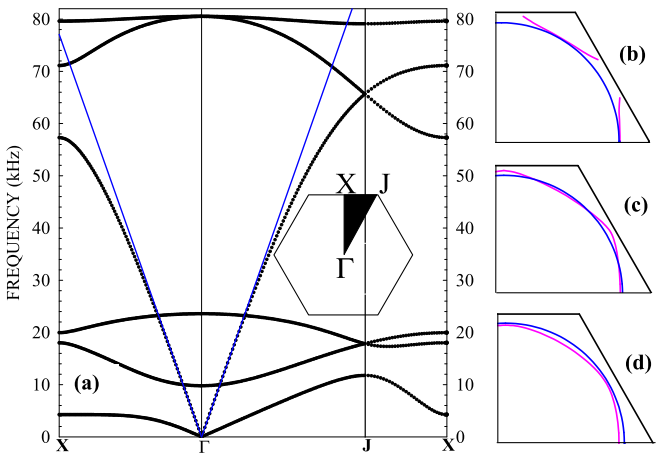

FIG. 2. (a) Dispersion curves in the first Brillouin zone, along the ΓJX path. The slope of the blue lines is the wave velocity in water. EFCs of the MWS represented in the right upper quadrant of the hexagonal Brillouin zone (the 3 other quadrants can be redrawn by symmetry). (b) 70.8 kHz, (c) 71.2 kHz, and (d) 71.6 kHz (pink). The blue circle corresponds to the EFC in water and the black lines to the Brillouin zone.

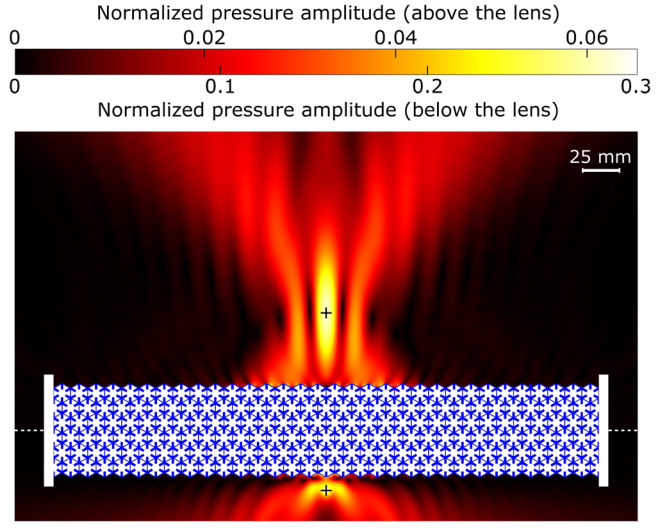

FIG. 3. Normalized (source level equal to 1 arbitrary unit) pressure field maps obtained for a focusing simulation. Aluminum surfaces are shown in blue. The source is located below the slab, and the focusing effect is observed above. Locations of the source and of the focus point are shown as black crosses. For clarity, different color maps are used below and above the slab.

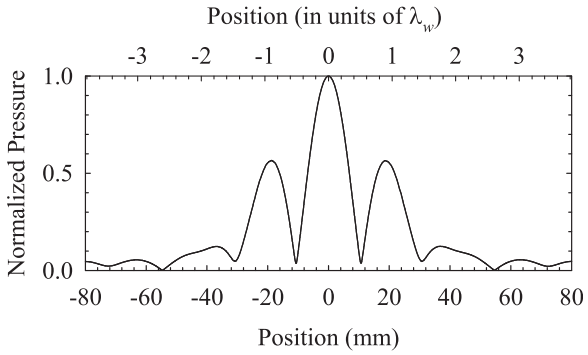

FIG. 4. Variation of the normalized (to the maximal value equal to 6% of the source amplitude) amplitude of the calculated pressure as a function of the position along a line parallel to the output side of the slab passing through the focal spot. $\lambda_w = 20.93$ mm is the wavelength in water at 71.2 kHz.

of the MWS slab at the operation frequency[19] deduced from the EFCs of Fig. 2(c). In summary, the water/MWS/water system exhibits perfect refraction index matching but rather poor impedance matching at 71.2 kHz.

The focusing power of flat lenses is usually measured through variations of the image pressure field along a line through the focal spot either parallel or perpendicular to the lens surface.[6] Lateral resolution is estimated from the half-width of the main lobe according to the Rayleigh criterion, yielding 0.53λ as can be observed in Fig. 4, very close to the resolution limit of 0.5λ. Nevertheless, it should be possible to improve the MWS lens resolution by optimizing the thickness and the width of the lens and by varying the distance of the source from the input side of the slab and its location in a direction parallel to the input side.[6]

Experimental measurements confirm our theoretical predictions. A MWS lens was assembled from 15 aluminum 5 mm thick plates. Each plate was cut using a water jet process based on the previously defined geometry. Subsequently the plates were stacked into a single MWS using glue. The manufactured MWS (Fig. 5) was 75 mm high and 265 mm wide with thickness between 58.1 mm and 60 mm. Measurements were performed in a water tank using a pair of transducers. The emitter-transducer was half inch diameter with focal length of 1.2 in., driven by three periods of 75 kHz sinusoidal electrical excitation. Its focal point (located 20 mm below the input side of the slab) serves as a point source in the experiment, enabling measurement of the lateral resolution. The acoustic wave transmitted through the MWS is detected using a half-inch diameter planar receiver-transducer, which is moved to scan the image area across a rectangular grid with

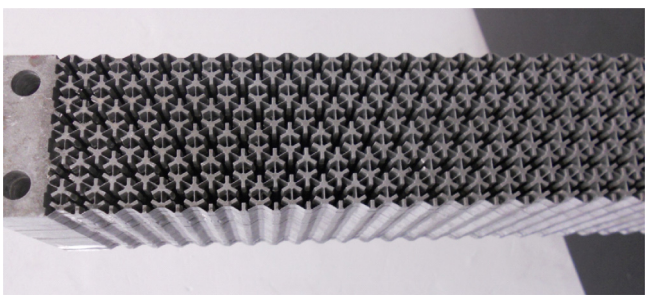

FIG. 5. The manufactured MWS lens.

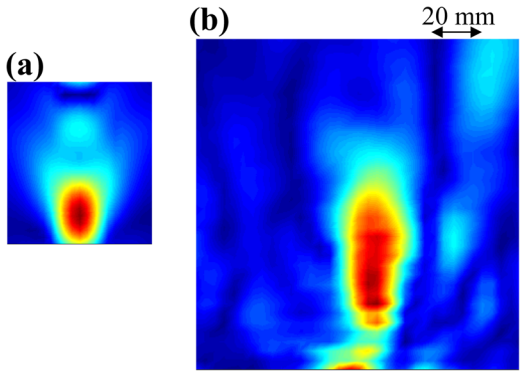

FIG. 6. Maps of the measured pressure field (in arbitrary units) around (a) the source and (b) the focal spot.

4 mm step. At each position the average over 128 sweeps is calculated from the temporal digitized signals, and image formation at particular frequencies is then obtained by fast Fourier transform. Time signals are filtered to eliminate echoes from the walls of the water tank in which the experimental setup is immersed. Figure 6 displays the corresponding pressure field around the source without the slab and around the focal spot at 81 kHz, which corresponds to the narrowest obtained image. The distance between the source and the image is 130 mm, e.g., approximately twice the thickness of the slab and the pressure level at the focal spot is 5% of the source level. These measured values agree quite well with their numerically predicted counterparts. Nevertheless, one observes a discrepancy between the experimental (81 kHz) and the theoretical frequency of 71.2 kHz. This discrepancy could be attributed to the manufacturing process of the sample. Indeed, the aluminum plates were glued together, and although the effect is difficult to quantify precisely, that may lead to changes in the physical characteristics of the sample. Moreover, some geometrical irregularities in the honeycomb network of metallic arms as well as at the interfaces between the MWS and surrounding water may occur. Finally we observed that during the experiments a small amount of water was infiltrated inside the MWS. These effects may have altered the MWS properties leading to different theoretical and observed operation frequencies. Figure 7 depicts the measured pressure along lines parallel to the interface passing through the source and the focal spot. The lateral resolution, estimated again by the half-width of the main lobe, is around

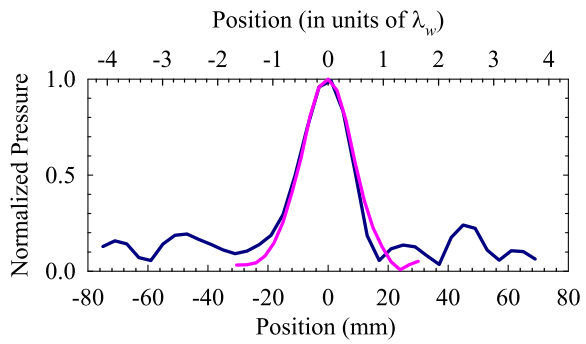

FIG. 7. Variation of the normalized (to the maximal value) amplitude of the measured pressure as a function of the position along a line parallel to the output side of the slab passing through the source (pink) or the focal spot (blue). $\lambda_w = 18.40$ mm is the wavelength in water at 81 kHz.

0.8λ for both the image spot and the source. Experimental measurements therefore unambiguously demonstrate the focusing capability of the MWS at an operation frequency of the order of a few tens of kHz. Nevertheless, better resolution should be obtained with a narrower source and by optimizing the experimental setup (thickness and width of the slab, location of the source with respect to the input side of the PC). Moreover due to the complete scalability of the results, the operation frequency can be shifted to much higher values by decreasing the unit cell size.

Theoretical and experimental investigations on the negative refraction properties and the focusing capability of an immersed slab made of a MWS are reported. The MWS can be depicted at a centimeter scale as a 2D periodic and porous network of interconnected aluminum arms and branches. Negative refraction of longitudinal waves is demonstrated around a few tens of kHz where index matching between surrounding water and the MWS is satisfied. Despite the low impedance matching at this frequency, the possibility of focusing longitudinal waves with a solid lens immersed in water was numerically and experimentally demonstrated. The MWS flat lens should be applied to image a fluid environment which is an important issue for applications in medical imaging devices.

The authors wish to thank ANR (Agence Nationale de la Recherche) and ONR (Office of Naval Research) for providing funding and FANO (Fédération Acoustique du Nord Ouest) - FR 3110 CNRS for its financial support in the manufacturing of the device, made in the Blois Institute of Technology (France).

[1]M. S. Kushwaha, Int. J. Mod. Phys. B **10**, 977 (1996).
[2]Y. Pennec, J. O. Vasseur, B. Djafari-Rouhani, L. Dobrzyński, and P. A. Deymier, Surf. Sci. Rep. **65**, 229 (2010).
[3]X. Zhang and Z. Liu, Appl. Phys. Lett. **85**, 341 (2004).
[4]M. Ke, Z. Liu, C. Qiu, W. Wang, and J. Shi, Phys. Rev. B **72**, 064306 (2005).
[5]A. Sukhovich, L. Jing, and J. H. Page, Phys. Rev. B **77**, 014301 (2008).
[6]J.-F. Robillard, J. Bucay, P. A. Deymier, A. Shelke, K. Muralidharan, B. Merheb, J. O. Vasseur, A. Sukhovich, and J. H. Page, Phys. Rev. B **83**, 224301 (2011).
[7]S. Peng, Z. He, H. Jia, A. Zhang, C. Qiu, M. Ke, and Z. Liu, Appl. Phys. Lett. **96**, 263502 (2010).
[8]L. Feng, X.-P. Liu, Y.-B. Chen, Z.-P. Huang, Y.-W. Mao, Y.-F. Chen, J. Zi, and Y.-Y. Zhu, Phys. Rev. B **72**, 033108 (2005).
[9]L. Feng, X.-P. Liu, M.-H. Lu, Y.-B. Chen, Y.-F. Chen, Y.-W. Mao, J. Zi, Y.-Y. Zhu, S.-N. Zhu, and N.-B. Ming, Phys. Rev. Lett. **96**, 014301 (2006).
[10]M.-H. Lu, C. Zhang, L. Feng, J. Zhao, Y.-F. Chen, Y.-W. Mao, J. Zi, Y.-Y. Zhu, S.-N. Zhu, and N.-B. Ming, Nat. Mater. **6**, 744 (2007).
[11]J. Christensen and F. J. G. de Abajo, Phys. Rev. Lett. **108**, 124301 (2012).
[12]B. Morvan, A. Tinel, A.-C. Hladky-Hennion, J. Vasseur, and B. Dubus, Appl. Phys. Lett. **96**, 101905 (2010).
[13]C.-Y. Chiang and P.-G. Luan, J. Phys.: Condens. Matter **22**, 055405 (2010).
[14]C. Croënne, D. Manga, B. Morvan, A. Tinel, B. Dubus, J. Vasseur, and A.-C. Hladky-Hennion, Phys. Rev. B **83**, 054301 (2011).
[15]A. N. Norris and A. J. Nagy, "Metal water: A metamaterial for acoustic cloaking," in *Proceedings of Phononics, Santa Fe, New Mexico, USA*, May 29-June 2 2011, pp. 112–113.
[16]A. N. Norris, Proc. R. Soc. A **464**, 2411 (2008).
[17]The density, the longitudinal, and transverse speeds of sound of aluminum are $\rho = 2700\,\mathrm{kg\,m^{-3}}, V_L = 6148\,\mathrm{m\,s^{-1}}$ and $V_T = 3097\,\mathrm{m\,s^{-1}}$, respectively. Losses are accounted for through an imaginary part of Young's modulus equal to 1% of the real part. ρ and V_L for water are $\rho = 1000\ \mathrm{kg\,m^{-3}}$ and $V_L = 1490\ \mathrm{m\,s^{-1}}$, respectively.
[18]P. Langlet, A. C. Hladky-Hennion, and J. N. Decarpigny, J. Acoust. Soc. Am. **98**, 2792 (1995).
[19]A. Sukhovich, Ph.D. dissertation, University of Manitoba, Winnipeg, Manitoba, 2007.